Inorganic Chemistry

ARTICLE

pubs.acs.org/IC

Intrinsically Fluorescent Glycoligands To Study Metal Selectivity

Ludivine Garcia,[†] Stéphane Maisonneuve,[‡] Jennifer Oudinet-Sin Marcu,[†] Régis Guillot,[†] François Lambert,[†,§] Juan Xie,[‡] and Clotilde Policar*[,†,§]

[§]Département de Chimie de l'ENS, Laboratoire des Biomolécules, UMR-CNRS 7203, Université Pierre et Marie Curie, 24 rue Lhomond, F-75231 Paris Cedex, France

[†]Institut de Chimie Moléculaire et des Matériaux d'Orsay, Bât. 420, Université Paris-Sud 11, F-91405 Orsay Cedex, France

[‡]PPSM, Institut d'Alembert, ENS Cachan, CNRS, 61 av. Président Wilson, F-94230 Cachan, France

Supporting Information

ABSTRACT: Glycoligands are a versatile family of ligands centered on a sugar platform and functionalized by Lewis bases. In this article, pentofuranoses were appended with the fluoroionophores 4-(pyridin-2′-yl)-1,2,3-triazol-1-yl and 4-(2′,1′,3′-benzothiadiazol-4′-yl)-1,2,3-triazol-1-yl using the "click-like" cycloaddition [2 + 3] of Huisgen catalyzed by copper(I). Their fluorescence properties were used to study metal cation complexation. A possible selective functionalization of furanoscaffolds allows the synthesis of "mixed" glycoligands with the successive insertion of these different fluoroionophores. The metal selectivity and the chelating behavior of these six resulting intrinsically fluorescent glycoligands were investigated. The change in the configuration at the carbon C3 of furanose did not influence either the metal selectivity or the binding constants. However, different selectivities and binding constants were found to depend on the nature of the fluoroionophore moieties. Overall, the triazolylbenzothiadiazolyl chelating group was shown to be less efficient than the triazolylpyridyl claw for complexation. Interestingly enough, the triazolylbenzothiadiazolyl claw, which fluoresces in the visible range, did not interfere in the binding and selectivity of the more efficient triazolylpyridyl claw. This study suggests that the triazolylbenzothiadiazolyl moiety could be used as an adequate fluorescent reporter to qualitatively monitor complexation of other moieties.

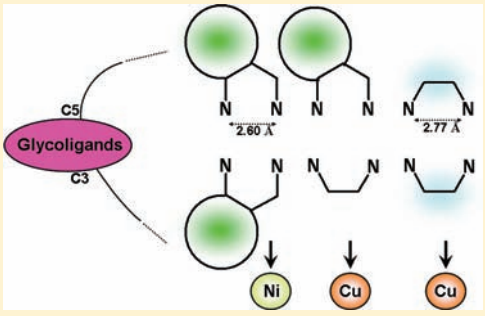

INTRODUCTION

Carbohydrates are promising scaffolds to tailor molecular diversity[1] because they are chiral and polyfunctional molecules with a broad variety of sizes, geometries, etc. Often used in organic chemistry as a central scaffold, the carbohydrate unit is scarcely involved in coordination chemistry as a platform except in a few examples[2] for asymmetric catalysis[3] and biomedical applications.[4] We have previously demonstrated that *glycoligands* could be obtained by appending Lewis bases on sugar scaffolds[5−8] and reported that a carbohydrate constraint platform can control the metal center properties of their corresponding complexes such as magnetism[9] or chirality.[10,11] In this article, we take advantage of the possible selective multifunctionalization of furanose scaffolds to introduce fluorescent coordinating moieties that were used as reporters to study metal complexation and determine metal selectivity.

The design of ligands able to selectively coordinate metal ions is of interest in many areas and is still a challenge today. With increasing interest in ecology, environment sciences are focused on the detoxification of industrial wastes, especially water treatment.[12,13] Metal selectivity is also of importance in medicinal chemistry. The design of therapeutic reagents[14] for the treatment of metal intoxication,[15] of antibiotics getting their activity after specific metal complexation,[16] and of complexes used as imaging agents[17] is a matter of fundamental importance.

An original way to analyze metal selectivity is to use fluoroionophores as appended chelating groups.[18] Therefore, many cation sensors have been introduced on various platforms such as diazatrithiacrown ether,[19] β-cyclodextrin,[20−22] conjugated systems,[23,24] peptides,[25] calixarenes,[22] and boron dipyrromethene.[26] Our strategy was to append fluoroionophores on a monosaccharide platform to obtain glycoligands with fluorescent properties, allowing the study of their metal selectivity.

In this work, the synthesis of three pairs of glycoligands is described by appending bidentate 4-(pyridin-2′-yl)-1,2,3-triazol-1-yl and/or 4-(2′,1′,3′-benzothiadiazol-4′-yl)-1,2,3-triazol-1-yl on two C3 epimeric pentofuranoses. The bidentate claws (see Schemes 1−3 for the coordinating atoms in bold italic) were chosen for their rigidity, their planarity, and their fluorescence properties.[20,21] Interestingly, glycoligands were shown to induce metal selectivity using fluorescence.

EXPERIMENTAL SECTION

Materials and Methods. All reagents employed (high-grade-purity materials) were commercially available and were used as supplied (Aldrich and Acros Organics). Chromatography was carried out using silica gel 60 Å (330−400 mesh). For thin-layer chromatography (TLC),

Received: April 28, 2011
Published: October 17, 2011

Scheme 1. Synthetic Pathways to L1 and L1′

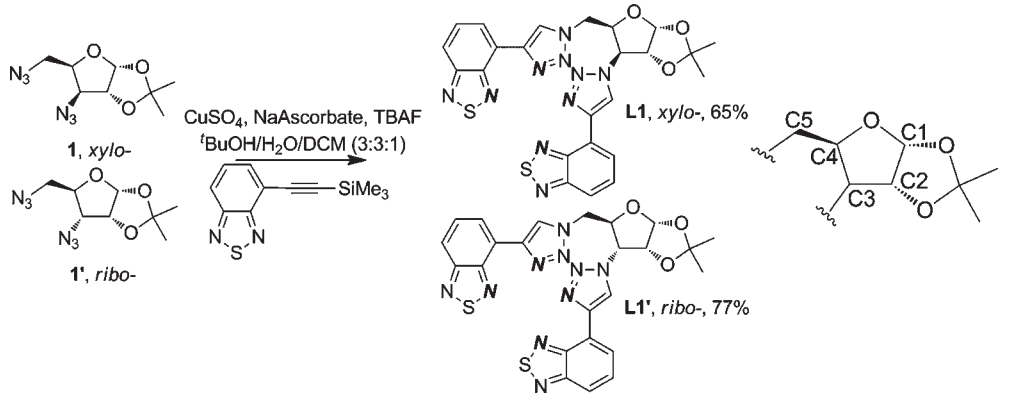

Scheme 2. Synthetic Pathways to L2 and L2′

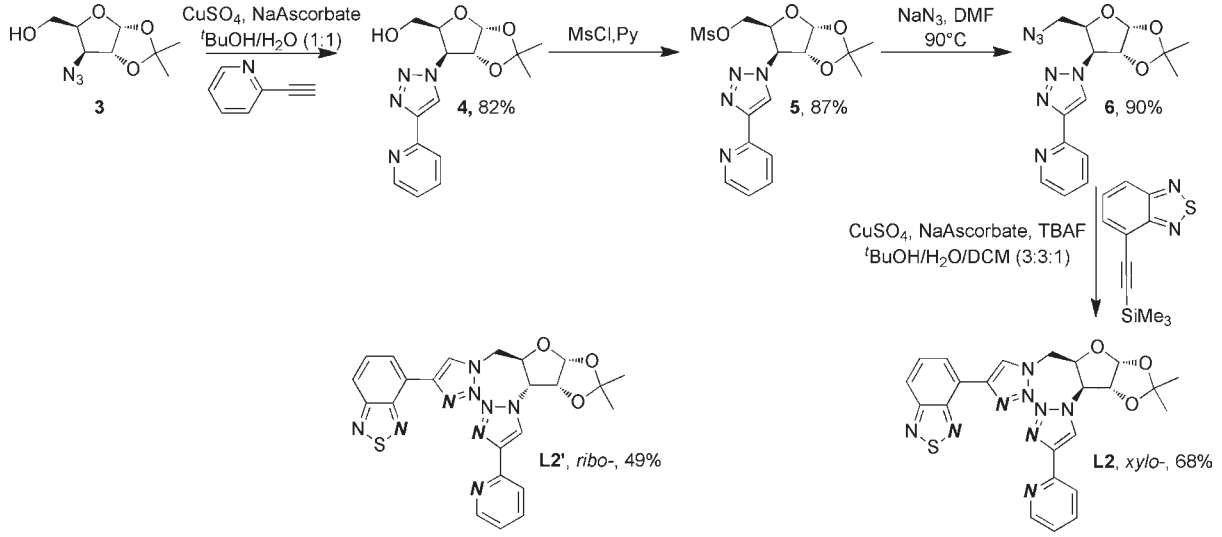

Merck silica gel 60 (layer: 0.20 mm) with fluorescent indicator UV_{254} on aluminum sheets was used. NMR spectra were obtained from dilute solutions in $CDCl_3$ at approximately 25 °C and recorded on Bruker DRX 250 (^{1}H, 250.13 MHz; ^{13}C, 62.90 MHz), Bruker DRX 300 (^{1}H, 300.132 MHz; ^{13}C, 75.475 MHz), and AV 360 (^{1}H, 360.113 MHz; ^{13}C, 90.559 MHz) spectrometers. The residual solvent signals were used as internal standards: $CDCl_3$ (^{1}H δ 7.27; ^{13}C δ 77.0). The resonance multiplicity is indicated as s (singlet), d (doublet), t (triplet), q (quartet), and m (multiplet). High-resolution electrospray spectra were recorded on a Finnigan MAT95S in a BE configuration. The syntheses of **1** and **1′** were previously published.[11] IR spectra were recorded on a Bruker IFS 66 FT-IR spectrometer in the range 4000−400 cm^{-1}. Electronic spectra of the ligands were recorded on a Cary-300-Bio spectrophotometer and carried out in aqueous solution at 20 °C.

Syntheses of L1 and L1′. To a solution of the diazido compounds **1** (**1′**)[11] (0.29 g, 1.19 mmol) in *t*-BuOH (15 mL) and CH_2Cl_2 (5 mL) was added sodium ascorbate (0.17 g, 0.83 mmol), copper(II) sulfate (0.66 g, 0.42 mmol), and water (15 mL). Tetrabutylammonium fluoride (0.75 g, 2.38 mmol) was used additionally to deprotect the alkyne. After a change of color (white to purple), 4-[(trimethylsilyl)ethyne]-2,1,3-benzothiadiazole (0.61 g, 2.63 mmol) was added. The mixture became orange. After being stirred overnight at room temperature, the mixture, which had become green, was extracted with 3 × 30 mL of CH_2Cl_2. The combined organic layers were then washed with a solution of ethylenediaminetetraacetic acid (EDTA; 0.1 mol L^{-1}) until the aqueous layer became colorless. The organic layer was dried over Na_2SO_4. After evaporation of the solvents and purification on silica gel (CH_2Cl_2/acetone, 9.5:0.5), the product of "click-like chemistry" was obtained.

Scheme 3. Representation of Glycoligands L3 and L3′

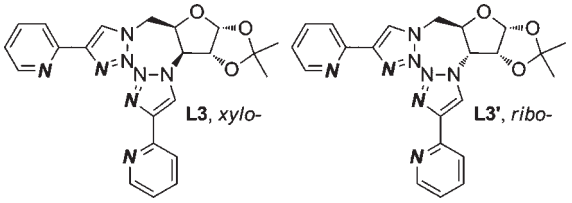

3,5-Bis[4-(2′,1′,3′-benzothiadiazol-4′-yl)-1,2,3-triazol-1-yl]-3,5-dideoxy-1,2-*O*-isopropylidene-α-D-xylofuranose (L1). Yellow powder. Yield: 65%. R_f = 0.8 (CH_2Cl_2/acetone, 9.5:0.5). ^{1}H NMR (250 MHz, $CDCl_3$): δ 8.75 (s, 1H, $H_{triazole}$), 8.60 (s, 1H, $H_{triazole}$), 8.52 (d, ^3J(H,H) = 7.0 Hz, 1H, H_{Ar}), 8.45 (d, ^3J(H,H) = 7.0 Hz, 1H, H_{Ar}), 7.93 (d, ^3J(H,H) = 8.7 Hz, 2H, 2 × H_{Ar}), 7.63−7.72

(m, 2H, 2 × H_{Ar}), 6.46 (d, ^3J(H,H) = 3.6 Hz, 1H, H1), 5.44 (d, ^3J(H,H) = 3.9 Hz, 1H, H3), 5.16−5.23 (m, 2H, H4, H2), 4.32−4.34 (m, 2H, H5, H5′), 1.59 (s, 3H, CH_3), 1.40 (s, 3H, CH_3). ^{13}C NMR (62.9 MHz, $CDCl_3$): δ 154.8, 151.3, 143.1, 142.9, 129.5, 125.4, 125.2, 125.0, 124.8, 122.8, 122.4, 120.9, 120.6, 112.8 ($C_{Q,isopropylidene}$), 105.6 (C1), 84.0 (C2), 77.5 (C4), 65.9 (C3), 48.4 (C5), 26.5 (CH_3), 26.0 (CH_3). IR (KBr): ν 3428 (C−H_{ar}), 3054, 2988 (C−H), 1641 (C═N), 1453, 1380, 1265, 1218, [1162, 1077, 1046, 1021] (aromatic nucleus), [890, 737] (C$_{ar}$−H) cm^{-1}. HRMS$^+$. Calcd for $C_{24}H_{21}O_3N_{10}S_2$ ([M + H]$^+$): *m/z* 561.1234. Found: *m/z* 561.1242.

3,5-Bis[4-(2′,1′,3′-benzothiadiazol-4′-yl)-1,2,3-triazol-1-yl]-3,5-dideoxy-1,2-*O*-isopropylidene-α-D-ribofuranose (L1′). Yellow powder. Yield: 77%. R_f = 0.8 (CH_2Cl_2/acetone, 9.5:0.5). ^{1}H NMR (300 MHz, $CDCl_3$): δ 8.96 (s, 1H, $H_{triazole}$), 8.85 (s, 1H, $H_{triazole}$), 8.40 (d, ^3J(H,H) = 6.8 Hz, 1H, H_{Ar}), 8.36 (d, ^3J(H,H) = 6.8 Hz, 1H, H_{Ar}), 7.95 (d, ^3J(H,H) = 8.7 Hz, 1H, H_{Ar}), 7.87 (d, ^3J(H,H) = 8.7 Hz, 1H, H_{Ar}), 7.65 (dd, ^3J(H,H) = 8.7 Hz, ^3J(H,H) = 6.8 Hz, 1H, H_{Ar}), 7.58 (dd, ^3J(H,H) = 8.7 Hz, ^3J(H,H) = 6.8 Hz, 1H, H_{Ar}), 6.03 (d, ^3J(H,H) = 3.0 Hz, 1H, H1), 5.26−5.29 (m, 1H, H3), 4.96−4.98 (m, 4H, H2, H4, H5, H5′), 1.59 (s, 3H, CH_3), 1.40 (s, 3H, CH_3). ^{13}C NMR (75.5 MHz, $CDCl_3$): δ 155.1, 151.6, 143.4, 143.3, 129.8, 129.6, 126.0, 125.4, 125.2, 124.5, 123.2, 123.1, 120.8, 120.6, 114.2 ($C_{Q,isopropylidene}$), 104.6 (C1), 78.8 (C2), 76.1 (C4), 62.4 (C3), 50.1 (C5), 26.6 (CH_3), 26.5 (CH_3). IR (KBr): ν 3423 (large, C−H_{ar}), 3057 (C−H_{ar}), 2987 (C−H), 2930 (C−H), 1644 (C═N), 1452, 1380, 1266, 1233, [1165, 1115, 1090, 1041] (aromatic nucleus), [887, 738] (C−H_{ar}) cm^{-1}. HRMS$^+$. Calcd for $C_{24}H_{21}O_3N_{10}S_2$ ([M + H]$^+$): *m/z* 561.1234. Found: *m/z* 561.1234.

Syntheses of 4 and 4′. To a solution of **3** (**3′**)[10] (0.62 g, 2.88 mmol) in *t*-BuOH (10 mL) was added sodium ascorbate (0.29 g, 1.44 mmol), copper(II) sulfate (0.11 g, 0.72 mmol), and water (10 mL). After a change of color (white to purple), 2-ethynylpyridine (0.33 g, 3.17 mmol) was added. The mixture became orange. After being stirred overnight at room temperature, the mixture, which had become green, was extracted with 3 × 10 mL of CH_2Cl_2. The organic layers were then washed with a solution of EDTA (0.1 mol L^{-1}) until the aqueous layer became colorless. The combined organic layers were dried over Na_2SO_4. After evaporation of the solvents, the product of "click-like chemistry" was obtained.

3-Deoxy-1,2-*O*-isopropylidene-3-(pyridin-2′-yl-1,2,3-triazol-1-yl)-α-D-xylofuranose (4). Yield: 82%. R_f = 0.2 (petroleum ether/EtOAc, 5:5). ^{1}H NMR (300 MHz, $CDCl_3$): δ 8.44 (d large, ^3J(H,H) = 4.9 Hz, 1H, H_{Py}), 8.25 (s, 1H, $H_{triazole}$), 8.09 (d, ^3J(H,H) = 7.9 Hz, 1H, H_{Py}), 7.72 (ddd, ^3J(H,H) ≈ ^3J(H,H) ≈ 7.7 Hz, ^4J (H,H) = 1.7 Hz, 1H, H_{Py}), 7.17 (dd, ^3J(H,H) = 7.4 Hz, ^4J(H,H) = 4.9 Hz, 1H, H_{Py}), 7.25 (d, ^3J(H,H) = 3.6 Hz, 1H, H1), 5.21 (d, ^3J (H,H) = 3.6 Hz, 1H, H2), 5.10 (d, ^3J(H,H) = 3.7 Hz, 1H, H3), 4.62−4.68 (m, 1H, H4), 3.59 (dd, ^2J(H,H) = 11.1 Hz, ^3J(H,H) = 5.8 Hz, 1H, H5), 3.08 (dd, ^2J(H,H) = 11.1 Hz, ^3J(H,H) = 7.5 Hz, 1H, H5′), 1.55 (s, 3H, CH_3), 1.34 (s, 3H, CH_3). ^{13}C NMR (75.5 MHz, $CDCl_3$): δ 149.6, 149.0, 147.6, 137.2, 123.2, 123.0, 120.5, 112.4 ($C_{Q,isopropylidene}$), 105.5 (C1), 83.5 (C2), 79.2 (C4), 65.6 (C3), 59.0 (C5), 26.5 (CH_3), 26.1 (CH_3). HRMS$^+$. Calcd for $C_{15}H_{19}O_4N_4$ ([M + H]$^+$): *m/z* 319.1401. Found: *m/z* 319.1415.

3-Deoxy-1,2-*O*-isopropylidene-3-(pyridin-2′-yl-1,2,3-triazol-1-yl)-α-D-ribofuranose (4′). Yield: 95%. R_f = 0.2 (petroleum ether/EtOAc, 5:5). ^{1}H NMR (300 MHz, $CDCl_3$): δ 8.44 (d large, ^3J(H,H) = 4.9 Hz, 1H, H_{Py}), 8.25 (s, 1H, $H_{triazole}$), 8.10 (d, ^3J(H,H) = 7.8 Hz, 1H, H_{Py}), 7.72 (ddd, ^3J(H,H) ≈ ^3J(H,H) ≈ 7.8 Hz, ^4J(H,H) = 1.7 Hz, 1H, H_{Py}), 7.17 (ddd, ^3J(H,H) = 7.4 Hz, ^3J(H,H) = 4.9 Hz, ^4J(H,H) = 0.9 Hz, 1H, H_{Py}), 6.25 (d, ^3J(H,H) = 3.6 Hz, 1H, H1), 5.22 (d, ^3J(H,H) = 3.7 Hz, 1H, H3), 5.10 (d, ^3J(H,H) = 3.6 Hz, 1H, H2), 4.63−4.68 (m, 1H, H4), 3.59 (dd, ^2J(H,H) = 11.1 Hz, ^3J(H,H) = 5.8 Hz, 1H, H5), 3.09 (dd, ^2J(H,H) = 11.1 Hz, ^3J(H,H) = 3.7 Hz, 1H, H5′), 1.55 (s, 3H, CH_3), 1.34 (s, 3H, CH_3). ^{13}C NMR (75.5 MHz, $CDCl_3$): δ 149.6, 149.0, 147.6, 137.2, 123.1, 123.0, 120.5, 112.4 ($C_{Q,isopropylidene}$), 105.5 (C1), 83.6 (C2), 79.2 (C4), 65.7 (C5), 59.1 (C3), 26.5 (CH_3), 26.1 (CH_3). HRMS$^+$. Calcd for $C_{15}H_{19}O_4N_4$ ([M + H]$^+$): *m/z* 319.1401. Found: *m/z* 319.1404.

Syntheses of 5 and 5′. To a solution of **4** (**4′**) (3.80 g, 17.7 mmol) in anhydrous pyridine (50 mL) at 0 °C was added dropwise mesyl chloride (2.43 g, 21.2 mmol). After being stirred overnight, the mixture was concentrated, redissolved in water/CH_2Cl_2 (50 mL/50 mL), and separated, and the aqueous layer was extracted with CH_2Cl_2 (2 × 50 mL). The organic layer was then dried (Na_2SO_4) and concentrated to afford the mesylated compound.

3-Deoxy-1,2-*O*-isopropylidene-5-*O*-methanesulfonyl-3-(pyridin-2′-yl-1,2,3-triazol-1-yl)-α-D-xylofuranose (5). Yield: 87%. R_f = 0.6 (petroleum ether/EtOAc, 5:5). ^{1}H NMR (360 MHz, $CDCl_3$): δ 8.57 (d large, ^3J(H,H) = 4.9 Hz, 1H, H_{Py}), 8.17 (s, 1H, $H_{triazole}$), 8.16 (d, ^3J(H,H) = 7.2 Hz, 1H, H_{Py}), 7.79 (ddd, ^3J(H,H) ≈ ^3J(H,H) ≈ 7.7 Hz, ^4J(H,H) = 1.5 Hz, 1H, H_{Py}), 7.26 (ddd, ^3J(H,H) = 7.4 Hz, ^3J(H,H) = 4.9 Hz, ^4J(H,H) = 1.5 Hz, 1H, H_{Py}), 6.31 (d, ^3J(H,H) = 3.6 Hz, 1H, H1), 5.26 (d, ^3J(H,H) = 3.9 Hz, 1H, H3), 5.03 (d, ^3J(H,H) = 3.6 Hz, 1H, H2), 4.83 (ddd, ^3J(H,H) ≈ ^3J(H,H) ≈ 6.1 Hz, ^3J(H,H) = 3.9 Hz, 1H, H4), 4.08 (dd, ^2J(H,H) = 11.0 Hz, ^3J(H,H) = 6.1 Hz, 1H, H5), 3.80 (dd, ^2J(H,H) = 11.0 Hz, ^3J(H,H) = 6.1 Hz, 1H, H5′), 2.94 (s, 3H, S−CH_3), 1.60 (s, 3H, CH_3), 1.37 (s, 3H, CH_3). ^{13}C NMR (62.9 MHz, $CDCl_3$): δ 149.2, 149.1, 148.3, 137.1, 123.3, 122.5, 120.4, 113.1 ($C_{Q,isopropylidene}$), 105.7 (C1), 83.9 (C2), 76.6 (C4), 65.6 (C5, C3), 37.4 (S−CH_3), 26.6 (CH_3), 26.1 (CH_3). HRMS$^+$. Calcd for $C_{16}H_{21}O_6N_4S_1$ ([M + H]$^+$): *m/z* 397.1176. Found: *m/z* 397.1179.

3-Deoxy-1,2-*O*-isopropylidene-5-*O*-methanesulfonyl-3-(pyridin-2′-yl-1,2,3-triazol-1-yl)-α-D-ribofuranose (5′). Yield: 91%. R_f = 0.4 (EtOAc). ^{1}H NMR (250 MHz, $CDCl_3$): δ 8.56 (d large, ^3J(H,H) = 4.1 Hz, 1H, H_{Py}), 8.28 (s, 1H, $H_{triazole}$), 8.11 (d, ^3J(H,H) = 7.9 Hz, 1H, H_{Py}), 7.75 (ddd, ^3J(H,H) ≈ ^3J(H,H) ≈ 7.7 Hz, ^4J(H,H) = 1.7 Hz, 1H, H_{Py}), 7.21 (ddd, ^3J(H,H) = 7.5 Hz, ^4J(H,H) = 4.9 Hz, ^5J(H, H) = 1.0 Hz, 1H, H_{Py}), 5.99 (d, ^3J(H,H) = 3.6 Hz, 1H, H1), 5.14 (dd, ^2J(H,H) = 10.0 Hz, ^3J(H,H) = 4.3 Hz, 1H, H3), 4.96 (dd, ^3J(H,H) ≈ ^3J(H,H) ≈ 3.9 Hz, 1H, H2), 4.75 (td, ^2J(H,H) = 10.0 Hz, ^3J(H,H) ≈ ^3J(H,H) ≈ 2.3 Hz, 1H, H4), 4.58 (dd, ^2J(H,H) = 11.9 Hz, ^3J(H,H) = 2.1 Hz, 1H, H5), 4.35 (dd, ^2J(H,H) = 11.9 Hz, ^3J(H,H) = 3.6 Hz, 1H, H5′), 3.04 (s, 3H, S−CH_3), 1.60 (s, 3H, CH_3), 1.33 (s, 3H, CH_3). ^{13}C NMR (62.9 MHz, $CDCl_3$): δ 149.6, 149.2, 148.3, 136.8, 122.9, 122.3, 120.2, 114.0 ($C_{Q,isopropylidene}$), 104.2 (C1), 78.5 (C3), 76.0 (C2), 66.7 (C5), 60.7 (C4), 37.4 (S−CH_3), 26.5 (CH_3), 26.2 (CH_3). HRMS$^+$. Calcd for $C_{16}H_{21}O_6N_4S_1$ ([M + H]$^+$): *m/z* 397.1176. Found: *m/z* 397.1182.

Syntheses of 6 and 6′. To a solution of **5** (**5′**) (1.98 g, 5.00 mmol) in *N*,*N*-dimethylformamide (30 mL) was added NaN_3 (1.30 g, 20.0 mmol). After 5 h at 90 °C, the solvent was evaporated and the residue was dissolved in a mixture of water/Et_2O (50 mL/50 mL). The layers were separated, and the aqueous one was extracted with 2 × 50 mL of Et_2O. Then the combined organic layers were washed with a saturated solution of NaCl, dried over $MgSO_4$, and evaporated to afford the corresponding azido compound.

5-Azido-3,5-dideoxy-1,2-*O*-isopropylidene-3-(pyridin-2′-yl-1,2,3-triazol-1-yl)-α-D-xylofuranose (6). Yield: 90%. R_f = 0.8 (petroleum ether/EtOAc, 5:5). ^{1}H NMR (360 MHz, $CDCl_3$): δ 8.55 (d large, ^3J(H,H) = 4.0 Hz, 1H, H_{Py}), 8.15 (d, ^3J(H,H) = 7.9 Hz, 1H, H_{Py}), 8.14 (s, 1H, $H_{triazole}$), 7.75 (td, ^3J(H,H) = ^3J(H,H) = 7.7 Hz, ^4J(H,H) = 1.8 Hz, 1H, H_{Py}), 7.22 (ddd, ^3J(H,H) = 7.5 Hz, ^4J(H,H) = 4.9 Hz, ^5J(H, H) = 1.1 Hz, 1H, H_{Py}), 6.27 (d, ^3J(H,H) = 3.6 Hz, 1H, H1), 5.16 (d, ^3J(H,H) = 3.8 Hz, 1H, H3), 5.01 (d, ^3J(H,H) = 3.6 Hz, 1H, H2), 4.62 (td, ^3J(H,H) ≈ ^3J(H,H) ≈ 6.7 Hz, ^3J(H,H) = 3.8 Hz, 1H, H4), 3.25 (dd, ^2J(H,H) = 12.8 Hz, ^3J(H,H) = 6.6 Hz, 1H, H5), 2.87 (dd, ^2J(H,H) = 12.8 Hz, ^3J(H,H) = 6.9 Hz, 1H, H5′), 1.57 (s, 3H, CH_3), 1.34 (s, 3H, CH_3). ^{13}C NMR (90.6 MHz, $CDCl_3$): δ 149.6, 149.4, 148.6, 136.9, 123.1, 122.4, 120.3, 112.7 ($C_{Q,isopropylidene}$), 105.6 (C1), 83.8 (C2), 77.5 (C4), 65.9 (C3), 48.9 (C5), 26.5 (CH_3), 26.1 (CH_3). HRMS$^+$. Calcd for $C_{15}H_{17}O_3N_7Na_1$ ([M + Na]$^+$): *m/z* 366.1285. Found: *m/z* 366.1291.

dx.doi.org/10.1021/ic200897v |*Inorg. Chem.* 2011, 50, 11353–11362

5-Azido-3,5-dideoxy-1,2-*O*-isopropylidene-3-(pyridin-2′-yl-1,2,3-triazol-1-yl)-α-D-ribofuranose (6′). Yield: 74%. R_f = 0.8 (petroleum ether/EtOAc, 5:5). ^{1}H NMR (250 MHz, $CDCl_3$): δ 8.52 (d large, ^3J(H,H) = 4.8 Hz, 1H, H_{Py}), 8.36 (s, 1H, $H_{triazole}$), 8.10 (d, ^3J(H,H) = 7.9 Hz, 1H, H_{Py}), 7.71 (ddd, ^3J(H,H) ≈ ^3J(H,H) ≈ 7.7 Hz, ^4J(H,H) = 1.7 Hz, 1H, H_{Py}), 7.16 (dd, ^3J(H,H) = 7.5 Hz, ^3J(H,H) = 5.9 Hz, 1H, H_{Py}), 5.96 (d, ^3J(H,H) = 3.5 Hz, 1H, H1), 5.10 (dd, ^3J(H,H) = 9.9 Hz, ^3J(H,H) = 4.4 Hz, 1H, H3), 4.90 (dd, ^3J(H,H) ≈ ^3J(H,H) ≈ 3.9 Hz, 1H, H2), 4.61 (dt, ^3J(H,H) = 9.9 Hz, ^3J(H,H) ≈ ^3J(H,H) ≈ 3.0 Hz, 1H, H4), 3.69 (dd, ^2J(H,H) = 13.8 Hz, ^3J(H,H) = 2.6 Hz, 1H, H5), 3.31 (dd, ^2J(H,H) = 13.8 Hz, ^3J(H,H) = 3.8 Hz, 1H, H5′), 1.57 (s, 3H, CH_3), 1.29 (s, 3H, CH_3). ^{13}C NMR (62.9 MHz, $CDCl_3$): δ 149.7, 149.2, 148.2, 136.8, 122.8, 122.1, 120.1, 113.9 ($C_{Q,isopropylidene}$), 104.1 (C1), 78.6 (C3), 77.2 (C2), 61.4 (C4), 49.8 (C5), 26.5 (CH_3), 26.1 (CH_3). HRMS$^+$. Calcd for $C_{15}H_{17}O_3N_7Na_1$ ([M + Na]$^+$): *m*/*z* 366.1285. Found: *m*/*z* 366.1291.

Syntheses of L2 and L2′. To a solution of **6** (**6′**) (1 equiv) in *t*-BuOH (7.0 mL for 0.50 g of the azido compound) and CH_2Cl_2 (2.0 mL for 0.50 g of the azido compound) was added sodium ascorbate (0.5 equiv), copper(II) sulfate (0.25 equiv), and water (7 mL for 0.50 g). After a change of color (white to purple), 4-[(trimethylsilyl)ethyne]-2,1,3-benzothiadiazole (1.1 equiv) was added. The mixture became orange. After being stirred overnight at room temperature, the mixture, which had become green, was extracted with 3 × 10 mL of CH_2Cl_2. The organic layers were then washed with a solution of EDTA (0.1 mol L^{-1}) until the aqueous layer became colorless. The combined organic layers were dried over Na_2SO_4. After evaporation of the solvents, the product of "click-like chemistry" was obtained.

3,5-Dideoxy-5-[4-(2′,1′,3′-benzothiadiazol-4′-yl)-1,2,3-triazol-1-yl]-3-(pyridin-2′-yl-1,2,3-triazol-1-yl)-1,2-*O*-isopropylidene-α-D-xylofuranose (L2). Yield: 68%. R_f = 0.4 (petroleum ether/EtOAc, 5:5). ^{1}H NMR (360 MHz, $CDCl_3$): δ 8.68 (s, 1H, $H_{triazole}$), 8.54 (d large, ^3J(H,H) = 4.2 Hz, 1H, H_{Ar}), 8.48 (d, ^3J(H,H) = 7.9 Hz, 1H, H_{Ar}), 8.32 (s, 1H, $H_{triazole}$), 8.19 (d, ^3J(H,H) = 7.9 Hz, 1H, H_{Ar}), 7.95 (d, ^3J(H,H) = 8.8 Hz, 1H, H_{Ar}), 7.79 (ddd, ^3J(H,H) ≈ ^3J(H,H) ≈ 7.7 Hz, ^4J(H,H) = 1.7 Hz, 1H, H_{Ar}), 7.69 (dd, ^3J(H,H) = 8.8 Hz, ^3J(H,H) = 7.1 Hz, 1H, H_{Ar}), 7.25 (ddd, ^3J(H,H) = 7.5 Hz, ^4J(H,H) = 4.9 Hz, ^5J(H,H) = 1.0 Hz, 1H, H_{Ar}), 6.39 (d, ^3J(H,H) = 3.6 Hz, 1H, H1), 5.38 (d, ^3J(H,H) = 3.8 Hz, 1H, H3), 5.05−5.10 (m, 2H, H2, H4), 4.39 (dd, ^2J(H,H) = 14.3 Hz, ^3J(H,H) = 5.7 Hz, 1H, H5), 4.21 (dd, ^2J(H,H) = 14.3 Hz, ^3J(H,H) = 6.9 Hz, H5′), 1.55 (s, 3H, CH_3), 1.37 (s, 3H, CH_3). ^{13}C NMR (75.5 MHz, $CDCl_3$): δ 155.1, 151.6, 149.4, 149.3, 148.7, 143.2, 137.0, 129.7, 125.3, 125.2, 123.2, 123.1, 123.0, 120.7, 120.4, 113.0 ($C_{Q,isopropylidene}$), 105.7 (C1), 84.2 (C3), 77.8 (C2), 66.1 (C4), 48.6 (C5), 26.5 (CH_3), 26.1 (CH_3). IR (KBr): ν 3055 (C−H_{ar}), 2986 (C−H), 1603 (C═N), 1423, 1265, [1079, 1033] (aromatic nucleus), [893, 738] (C−H_{ar}) cm^{-1}. HRMS$^+$. Calcd for $C_{23}H_{21}O_3N_9SNa$ ([M + Na]$^+$): *m*/*z* 526.1386. Found: *m*/*z* 526.1370.

3,5-Dideoxy-5-[4-(2′,1′,3′-benzothiadiazo-4′-yl)-1,2,3-triazol-1-yl]-3-(pyridin-2′-yl-1,2,3-triazol-1-yl)-1,2-*O*-isopropylidene-α-D-ribofuranose (L2′). Yield: 49%. R_f = 0.3 (petroleum ether/EtOAc, 5:5). ^{1}H NMR (360 MHz, $CDCl_3$): δ 8.84 (s, 1H, $H_{triazole}$), 8.58 (d large, ^3J(H,H) = 4.1 Hz, 1H, H_{Ar}), 8.47 (dd, ^3J(H,H) = 7.0 Hz, ^4J(H,H) = 0.9 Hz, 1H, H_{Ar}), 8.43 (s, 1H, $H_{triazole}$), 8.13 (d, ^3J(H,H) = 7.9 Hz, 1H, H_{Ar}), 7.93 (dd, ^3J(H,H) = 8.8 Hz, ^4J(H,H) = 0.9 Hz, 1H, H_{Ar}), 7.77 (ddd, ^3J(H,H) = ^3J(H,H) = 7.7 Hz, ^4J(H,H) = 1.7 Hz, 1H, H_{Ar}), 7.66 (dd, ^3J(H,H) = 8.8 Hz, ^3J(H,H) = 7.1 Hz, 1H, H_{Ar}), 7.23 (ddd, ^3J(H,H) = 7.6 Hz, ^4J(H,H) = 4.8 Hz, ^5J(H,H) = 0.9 Hz, 1H, H_{Ar}), 5.97 (d, ^3J(H,H) = 3.3 Hz, 1H, H1), 5.06−5.11 (m, 1H, H3), 4.86−4.92 (m, 4H, H5, H5′, H4, H2), 1.62 (s, 3H, CH_3), 1.34 (s, 3H, CH_3). ^{13}C NMR (75.5 MHz, $CDCl_3$): δ 155.0, 151.5, 149.7, 149.2, 148.4, 143.1, 136.8, 129.6, 125.8, 125.2, 123.1, 122.9, 122.5, 120.5, 120.2, 114.2 ($C_{Q,isopropylidene}$), 104.4 (C1), 78.7 (C2), 76.3 (C3), 62.2 (C4), 50.0 (C5), 26.6 (CH_3), 26.3 (CH_3). IR (KBr): ν 3054 (C−H_{ar}), 2987 (C−H), 2947 (C−H), 1604 (C═N), 1422, 1265, 1038 (aromatic nucleus), [895, 739] (H_{ar}) cm^{-1}. HRMS$^+$. Calcd for $C_{23}H_{21}O_3N_9SNa$ ([M + Na]$^+$): *m*/*z* 526.1386. Found: *m*/*z* 526.1390.

X-ray Structure Analyses. Crystals of **L1** and **L2′** were grown from concentrated $CHCl_3$ solutions of the respective compounds via slow evaporation. The diffraction intensities of crystals were collected with graphite-monochromatized Mo Kα radiation. Data collection and cell refinement were carried out using a Bruker Kappa X8 APEX II diffractometer. The temperature of the crystal was maintained at the selected value (100 K) by means of a 700 Series Cryostream cooling device to within an accuracy of ±1 K. Intensity data were corrected for Lorenz-polarization and absorption factors. The structures were solved by direct methods using *SHELXS-97*[27] and refined against F^2 by full-matrix least-squares methods using *SHELXL-97*[28] with anisotropic displacement parameters for all non-H atoms. All calculations were performed by using the Crystal Structure crystallographic software package *WINGX*. The structure was drawn using ORTEP3. H atoms were located on a difference Fourier map and introduced into the calculations as a riding model with isotropic thermal parameters.

Fluorescence. Stock solutions of all of the glycoligands (C = 10^{-3} mol L^{-1}) and of all the metal perchlorate salts ($C = 10^{-2}$ mol L^{-1}) were prepared in dimethyl sulfoxide (DMSO). Fluorescence emission spectra were recorded on a Jobin-Yvon Spex Fluorolog 1681 spectrofluorimeter. The fluorescence quantum yield (ϕ_F) was determined by the standard method using 1.0 × 10^{-5} M quinine sulfate in a 0.5 N H_2SO_4 solution as references for **L1**, **L1′**, **L2**, and **L2′**. The refractive index was taken into account in the measurement. The titration experiment was conducted in acetonitrile for **L1**, **L1′**, **L2**, **L2′**, **L3**, and **L3′**. The fluorescence spectra were corrected from the absorbance A at the excitation wavelength by a multiplied factor of $1/(1 - 10^{-A(260\ nm)})$ and from the fluorescence spectra of the solvent. For the competitive experiments, the fluorescence profiles were determined using the area under the curve of fluorescence. Evolution of the full fluorescence area from the ligands **L1**, **L1′**, **L2**, and **L2′** as a function of the copper(II) or nickel(II) concentration contains information on the stability constant of the complex through the following equation:[20,29]

$$Y(C_M) = Y_0 + 0.5(Y_{lim} - Y_0)\{1 + C_M/C_L + 1/KC_L - [(1 + C_M/C_L + 1/KC_L)^2 - 4C_M/C_L]^{1/2}\} \quad (1)$$

where Y designates the fluorescence intensity of a C_L-concentrated solution ($C_L = 8 \times 10^{-6}$ mol L^{-1}) of the ligand as a function of the concentration C_M of added cation. Y_0 and Y_{lim} are the fluorescence area values for $C_M = 0$ and for full complexation, respectively. K is the stability constant of the 1:1 complex.

For titration of **L3** and **L3′**, absorption and fluorescence spectra were globally analyzed using the *SPECFIT* Global Analysis System V3.0 for a 32-bit Window system.[22,30] This software uses singular value decomposition and nonlinear regression modeling by the Levenberg−Marquardt method.[31]

RESULTS AND DISCUSSION

Glycoligands **L1**, **L1′**, **L2**, **L2′**, **L3**, and **L3′** (Schemes 1−3) were designed as fluoroionophores, and their fluorescent properties were used to study complexation.[20,21] The syntheses of **L3** and **L3′** have been previously described.[11] **L1** and **L1′** bear two 1-triazolyl-4-benzothiadiazolyl moieties, while **L2** and **L2′** bear 1-triazolyl-2-pyridyl and 1-triazolyl-4-benzothiadiazolyl moieties (Schemes 1 and 2).

Synthesis of L1, L1′, L2, and L2′. **L1** and **L1′** were synthesized using the copper(I)-catalyzed Huisgen 1,3-dipolar cycloaddition[32] on 3,5-diazido-3,5-dideoxy-1,2-isopropylidene-α-D-furanoses **1** and **1′** (Scheme 1). As shown in the case of the mixed **L2** and

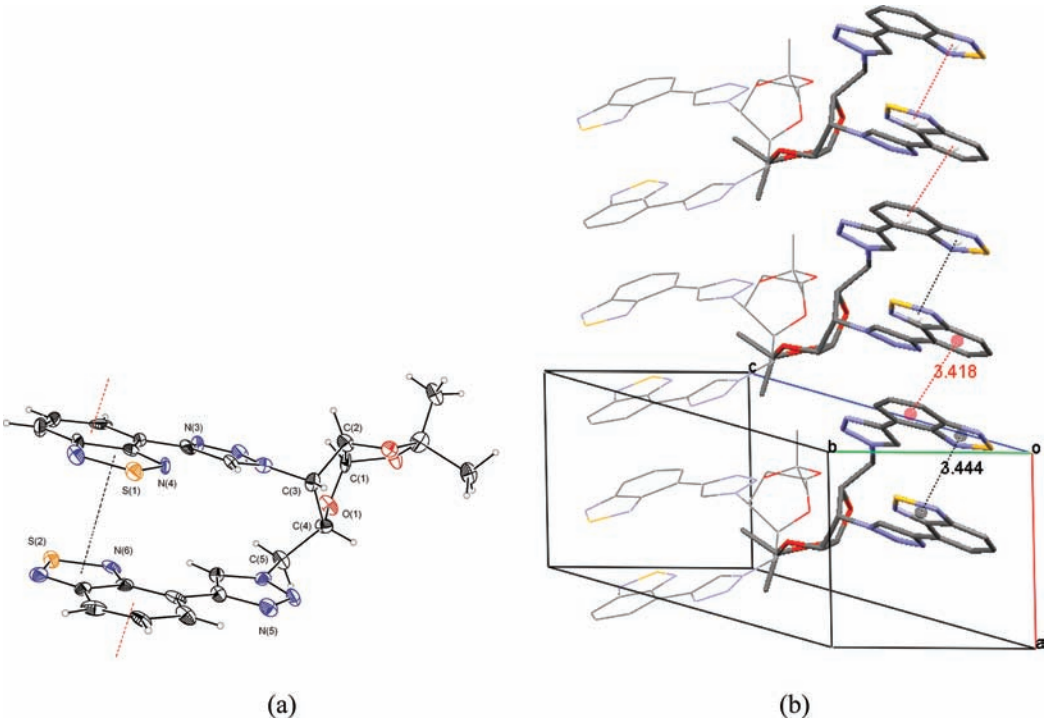

Figure 1. (a) ORTEP view of the molecule of **L1**, showing the atom-numbering scheme. Displacement ellipsoids are drawn at the 30% probability level, and H atoms are shown as small spheres of arbitrary radii. (b) View of part of the crystal structure of **L1** showing the formation of two [100] chains built from intra- and intermolecular $\pi-\pi$ interactions (centroids of the rings are denoted by small spheres).

L2′ described in Scheme 2, it is possible to append selectively different chelating groups on the C3 and C5 positions. In the first step, **3** (**3′**) was involved in a Huisgen 1,3-dipolar cycloaddition[33] catalyzed by copper(I) to form the 1-triazolyl-2-pyridyl claw of **4** (**4′**) as previously published.[21] Then, after mesylation of **4** (**4′**) and substitution by an azide on position C5, **L2** (**L2′**) was obtained by a second Huisgen 1,3-dipolar cycloaddition.[20]

The syntheses of these six ligands (L*n*/L*n*′, *n* = 1−3) showed that the Huisgen 1,3-dipolar cycloadditions applied on various positions of sugar derivatives can tailor the molecular diversity.[34,35]

X-ray Structures of Ligands L1 and L2′. Single crystals of **L1** and **L2′**, suitable for X-ray diffraction, were grown by slow evaporation of chloroform solutions. The ellipsoid plots of **L1** and **L2′** are shown in Figures 1a and 2a, respectively. The X-ray structure of **L3′** was previously described.[11] **L1**, **L2′**, and **L3′** crystallize in the monoclinic space group $P2_1$. The crystal packing of **L1** and **L2′** shows a rich supramolecular chemistry. Figure 1b presents the intra- and intermolecular overlapping of the triazolylbenzothiadiazolyl claw in **L1**.[36] The angle and distance between the two adjacent planes and centroids of the intramolecular thiadiazole rings are 2.8° and 3.44 Å, respectively (Figure 1b). Similar characteristics were found for the intermolecular π stacking between the two adjacent benzene rings of benzothiadiazole, that is, 2.8° and 3.42 Å (Figure 1b). These results indicate strong $\pi-\pi$ intra- and intermolecular interactions.

The crystal packing of **L2′** (Figure 2b) showed only $\pi-\pi$ intermolecular interactions between pyridine and the benzene rings of benzothiadiazole with an angle of 8.5° and a distance of 3.65 Å between respectively the planes and centroids of the rings (see Figure 2).

Similar $\pi-\pi$ interactions were observed in the case of **L3′**, as previously reported.[11] These $\pi-\pi$ interactions have been previously determined to have an important stabilizing effect in water and to participate in control of the nuclearity and preorganization of the ligand.[11]

UV−Visible and Fluorescence Properties of the Ligands. The absorption spectra of the six ligands were performed in acetonitrile. **L1** (**L1′**) exhibits n−π^* absorption bands at 358 nm and three resolved bands at 302, 308, and 316 nm, characteristics of the triazolylbenzothiadiazolyl group.[20,21,37,38] **L3** (**L3′**) has a UV pattern similar to that previously reported in water:[11] a large absorption band at 280 nm characteristic of the n−π^* absorption band of 1-triazolyl-2-pyridyl.[24] It is noteworthy that **L2** and **L2′** present absorption bands of both the triazolylpyridyl and triazolylbenzothiadiazolyl chelating groups, with an extinction coefficient scaled by a factor of $^1/_2$, as was expected from their design (Figure 3).

Fluorescence spectra in acetonitrile are reported in Tables 1 and 2 and in Figure 4. Interestingly enough, the 1-triazolyl-4-benzothiadiazolyl moiety in **L1** and **L2** (**L1′** and **L2′**) showed a unique fluorescence emission band in the visible range around 460−470 nm upon excitation at 358 or 368 nm (Table 1 and Figure 4), as was previously published.[20] On the contrary, compounds **L3** and **L3′** exhibited two fluorescence emission bands, revealing in acetonitrile the presence of a monomer species around 320 nm and of an excimer species at 370 nm upon excitation at 260 nm, as was previously published in water.[11] What is noteworthy is that the fluorescence areas, at the same concentration, of **L2** and **L2′** are about two times higher than those of **L1** and **L1′**, while they are designed with only one 1-triazolyl-4-benzothiadiazolyl claw (Figure 4).

Solvatofluorochromism of **L1**, **L1′**, **L2**, and **L2′** was also investigated. As shown in Figure 5, compounds **L1** and **L2** displayed negative solvatofluorochromism with a decrease in the fluorescence efficiency with increasing solvent polarity. A red shift of about 50 nm

dx.doi.org/10.1021/ic200897v |*Inorg. Chem.* 2011, 50, 11353–11362

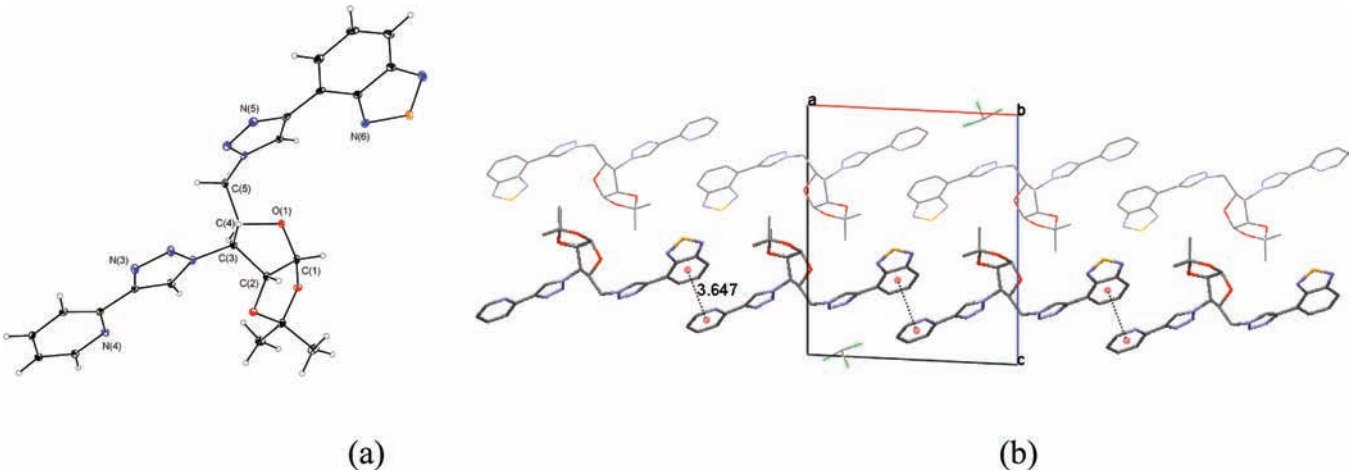

Figure 2. (a) ORTEP view of the molecule of **L2′**, showing the atom-numbering scheme. Displacement ellipsoids are drawn at the 30% probability level, and H atoms are shown as small spheres of arbitrary radii (solvent molecules are omitted for clarity). (b) View of part of the crystal structure of **L2′** showing the formation of two [010] chains built from intermolecular $\pi-\pi$ interactions (centroids of the rings are denoted by small spheres).

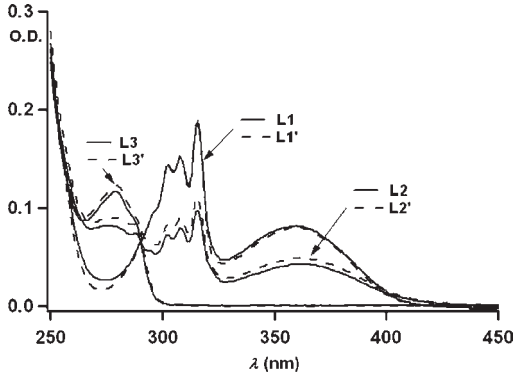

Figure 3. Absorption spectra of **L1**, **L1′**, **L2**, **L2′**, **L3**, and **L3′** in acetonitrile ($C = 8 \times 10^{-6}$ mol L^{-1}).

Table 1. Spectroscopic Data and Experimental Conditions of Excitation for L1, L1′, L2, L2′, L3, and L3′ in Acetonitrile

	L1	L1′	L2	L2′	L3	L3′
λ_{max} (nm)	358	358	368	368	280	280
ε (L mol^{-1} cm^{-1})	10 705	8980	5545	5568	8533	8371
λ_{ex} (nm)	358	358	368	368	260[a]	260[a]
λ_{em} (nm)	460	460	470	470	320, 370	320, 370

[a] λ_{ex} is different from λ_{max} for more acute values of the fluorescence intensity by avoiding emission of the lamp to interfere with our signal.

is observed for emission of **L1**, **L1′**, **L2**, and **L2′** from around 450 nm in acetonitrile to 500 nm in water. The fluorescence quantum yields (ϕ_F) for all of the ligands are reported in Table 2. Interestingly enough, the highest quantum yield was obtained for the glycoligands **L2** and **L2′** with the mixed fluoro units.

Application of Intrinsically Fluorescent Ligands to the Study of Metal Selectivity. Fluorescent coordinating moieties are of interest because they provide a straightforward means to study complexation properties and selectivity. Indeed, their photophysical properties may be modified upon complexation of metal cations (quenching, exaltation, or emission shift). Therefore, fluoroionophores can be used to gain insight into

Table 2. Quantum Yields for L1, L1′, L2, L2′, L3, and L3′ at $C = 8$ μmol L^{-1} in Water, Ethanol (EtOH), Acetonitrile, CH_2Cl_2, and DMSO with Reference to Naphthalene in a Nondeoxygenated Cyclohexane Solution for L3 and L3′ and with Reference to Quinine Sulfate in a Sulfuric Acid/Water Solution for L1, L1′, L2, and L2′

	ϕ_F (%)					
solvent	L1	L1′	L2	L2′	L3	L3′
H_2O	8.4	3.6	74	94	20[a]	20[a]
EtOH	38	30	78	80	7.0	9.0
CH_3CN	32	25	71	68	0.61	1.1
CH_2Cl_2	44	39	83	74	2.3	1.1
DMSO	45	29	54	64	0.13	0.21

[a] Mixture of H_2O/DMSO (85:15).

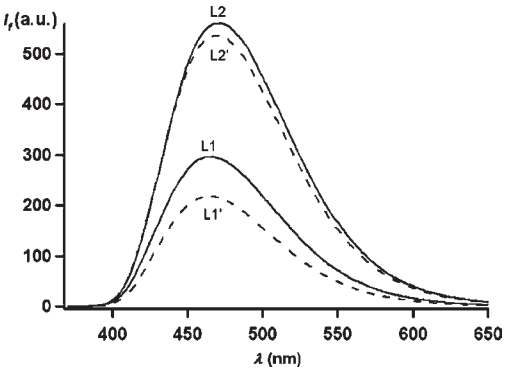

Figure 4. Fluorescence spectra of **L1**, **L1′**, **L2**, and **L2′** in acetonitrile ($C = 8 \times 10^{-6}$ mol L^{-1}). λ_{ex}= 358 nm for **L1** and **L1′** and 368 nm for **L2** and **L2′**.

the binding properties. To study the metal selectivity, competitive experiments have to be performed involving a series of metal cations. The first step is to identify, in this series, the cations that induce a change in the photophysical properties of the fluorescent moiety, for example, a quenching [see Figure 6, line a, for **L1** and

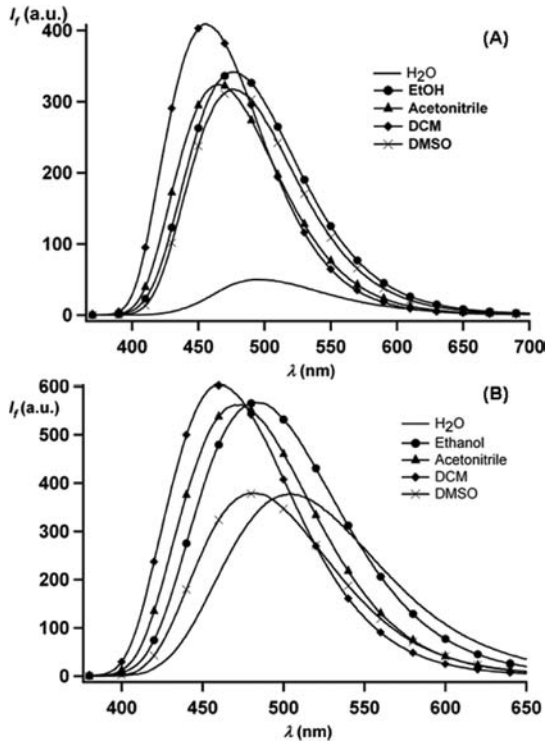

Figure 5. Fluorescence spectra of **L1** (A) and **L2** (B) in water, EtOH, acetonitrile, CH_2Cl_2, and DMSO. λ_{ex} = 358 nm (A) and 368 nm (B).

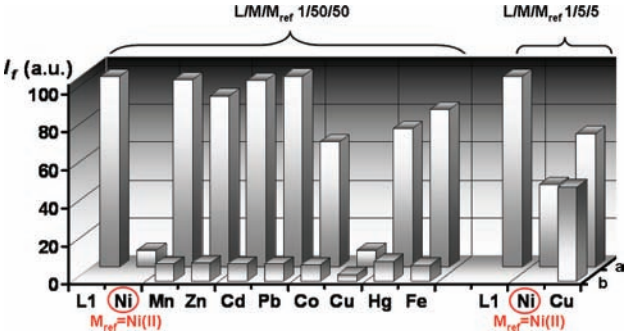

Figure 6. Fluorescence intensity change profiles of **L1** ($C = 8 \times 10^{-6}$ mol L^{-1}) in acetonitrile with selected cations ($C = 4 \times 10^{-4}$ mol L^{-1}, 50 equiv, or $C = 4 \times 10^{-5}$ mol L^{-1}, 5 equiv) in (a) the absence or (b) the presence of Ni^{II} ($C = 4 \times 10^{-4}$ mol L^{-1}, 50 equiv, or $C = 4 \times 10^{-5}$ mol L^{-1}, 5 equiv). λ_{ex} = 358 nm.

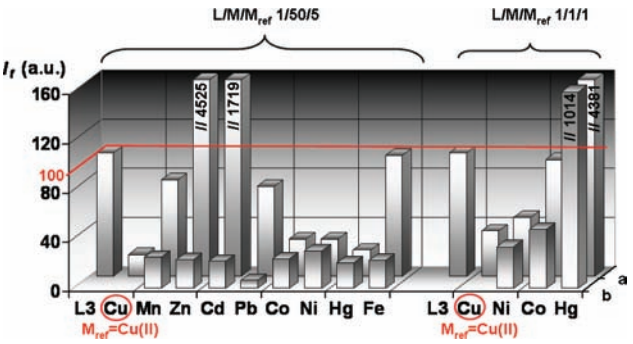

Figure 7. Fluorescence intensity change profiles of **L3** ($C = 8 \times 10^{-6}$ mol L^{-1}) in acetonitrile with selected cations ($C = 4 \times 10^{-4}$ mol L^{-1}, 50 equiv, or $C = 8 \times 10^{-6}$ mol L^{-1}, 1 equiv) in (a) the absence or (b) presence of Cu^{II} ($C = 4 \times 10^{-5}$ mol L^{-1}, 5 equiv, or $C = 8 \times 10^{-6}$ mol L^{-1}, 1 equiv). λ_{ex} = 260 nm.

the quenching of copper(II) and nickel(II)]. Then, a qualitative study by successive addition of the cations to a solution of the ligand led to the determination of the preferred cation, that is, the one that imposes its photophysical effect. In a second step, the competitive diagram is obtained by the addition of M_{ref} to a solution of L + M (line b).

This is exemplified below in the case of **L1**. Among a series of divalent cations including Pb^{II}, Cd^{II}, Zn^{II}, Mn^{II}, Ni^{II}, Fe^{II}, Hg^{II}, Co^{II}, and Cu^{II} at a ratio M/L of 50:1 in acetonitrile, Cu^{II} and Ni^{II} exhibit the most important quenching of fluorescence (Figure 6, line a). Other metal ions exhibit relatively weak fluorescence quenching, indicating either the absence of complexation or a complexation inducing no fluorescence change. To discriminate between Ni^{II} and Cu^{II} ions, a lower 5:1 M/L ratio was assayed: at a 5:1 M/L ratio, Ni^{II} was shown to induce a higher quenching. It was thus selected as the metal cation of reference.

The results of the competitive experiment are shown in Figure 6, line b. This indicates an inhibition of fluorescence by Ni^{II} at a ratio $L/M/M_{ref}$ of 1:50:50 for M = Pb^{II}, Cd^{II}, Zn^{II}, Mn^{II}, Ni^{II}, Fe^{II}, Hg^{II}, and Co^{II} (except Cu^{II}). In all possible cases (the absence of complexation of M by L or complexation of M by L inducing no photophysical change), the inhibition of fluorescence by Ni^{II} indicates Ni^{II} coordination and is the signature of a preference for Ni^{II} over other cations. In the case of Cu^{II}, the inhibition by Ni^{II} was obtained at a $L/Cu^{II}/Ni^{II}$ ratio of 1:5:5, indicating again a preference coordination of Ni^{II} over Cu^{II} but less pronounced.

Metal competitive experiments were also carried out for **L1′** in acetonitrile showing a similar competitive diagram (Figure S2 in the Supporting Information). **L1** and **L1′** present metal selectivity for Ni^{II} similar to that previously reported for the triazolylbenzothiadiazolyl claw.[20] For **L2** and **L2′**, selectivity in favor of Cu^{II} was observed for only 5 equiv of Cu^{II} versus 50 equiv of the previously mentioned metal cations (Figures S3 and S4 in the Supporting Information). Although 50 equiv of Ni^{II}, Co^{II}, and Hg^{II} induced a fluorescent change upon complexation with **L2** and **L2′**, a ratio of 1:1 M^{II}/Cu^{II} with M = Ni^{II}, Co^{II}, or Hg^{II} showed that the selectivity is in favor of Cu^{II}.

In the particular cases of **L3** and **L3′**, the competitive diagram revealed a different behavior upon complexation with exaltation of the fluorescence for some of the cations (Figure 7). Upon the addition of 50 equiv of the selected divalent cations to the acetonitrile solution of **L3**, the fluorescence emission was not affected by Fe^{II}, slightly quenched by Pb^{II} and Mn^{II}, strongly quenched by Cu^{II}, Ni^{II}, Co^{II}, and Hg^{II} but exalted for Zn^{II} and Cd^{II} (Figure 7, line a).[39]

The selectivity toward Cu^{II} was established by the competition experiment by adding 5 equiv of Cu^{II} to the previous metal ion−ligand mixtures ($L/M/M_{ref}$, 1:50:5; Figure 7, line b). The emission was similarly quenched as in the presence of Cu^{II} alone. In the case of Ni^{II}, Co^{II}, and Hg^{II}, the fluorescence emission in a ratio of 1:1 with Cu^{II} was determined (see Figure 7). This indicated a preference of **L3** for Cu^{II}. It is worth noting that 50 equiv of Hg^{II} quenched the fluorescence of **L3**, whereas 1 equiv exalted the fluorescence (Figure 7). Similar results were obtained for **L3′** (Figure S5 in the Supporting Information).

A qualitative selectivity order was established from the change of fluorescence upon the addition of different metal cations

dx.doi.org/10.1021/ic200897v |Inorg. Chem. 2011, 50, 11353–11362

Table 3. Summarized Cation Selectivities and Association Constants for L1, L1′, L2, L2′, L3, and L3′ in Acetonitrile

Ln	thermodynamically selective of	log β for the cation M (M:L= 1:1)	order of the fluorescence selectivity
L1	Ni^{II}	4.47 ± 0.02	$Ni^{II} > Cu^{II}$
L1′	Ni^{II}	4.69 ± 0.03	$Ni^{II} > Cu^{II}$
L2	Cu^{II}	6.5 ± 0.1	$Cu^{II} > Ni^{II} > Co^{II} > Hg^{II}$
L2′	Cu^{II}	7.3 ± 0.8	$Cu^{II} > Ni^{II} \approx Co^{II} > Hg^{II}$
L3	Cu^{II}	8.54 ± 0.03[a]	$Cu^{II} > Ni^{II} > Hg^{II} > Co^{II}$
L3′	Cu^{II}	7.8 ± 0.2[b]	$Cu^{II} > Ni^{II} \approx Co^{II} > Hg^{II}$

[a] For **L3**, $\log\beta(ML_2) = 9.7 \pm 0.2$ and $\log\beta(M_2L_2) = 17.30 \pm 0.05$. [b] For **L3′**, $\log\beta(ML_2) = 15.3 \pm 0.2$ and $\log\beta(M_2L_2) = 22.7 \pm 0.4$.

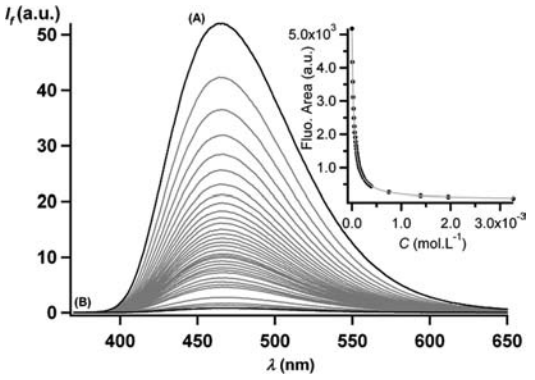

Figure 8. Fluorescence spectra obtained during titration of **L1** in acetonitrile ($C = 8 \times 10^{-6}$ mol L^{-1}) with $Ni(ClO_4)_2$ (from 0 to 400 equiv). λ_{ex} = 358 nm. Inset: fluorescence area (●); fitting curve (−) using eq 1. R^2 = 0.9993.

(see Table 3) by considering the values of the ratio between the fluorescence intensity obtained for the L + M solution and the L + M + M_{ref} solution.

All of the compounds, in the presence of 50 equiv of Cu^{II} or Ni^{II}, showed strong fluorescence quenching, like most of the reported Cu^{II} and Ni^{II} fluorescent sensors, because of their paramagnetic nature.[25,26,40−43] According to Table 3, modulation of the chelating claws leads to various metal cation selectivities. The C3 configuration does not affect the selectivity. **L1** and **L1′**, bearing two triazolylbenzothiadiazolyl claws, were determined to be selective for Ni^{II} and **L3** and **L3′**, bearing two triazolylpyridyl claws, for Cu^{II}. This may correspond to a size selectivity (ionic radii for Cu^{II} and Ni^{II} are respectively 0.57 and 0.49 Å for a tetradentate coordination sphere[44]) because the triazolylbenzothiadiazole claw displays a distance between the two N donors (see Schemes 1−3 coordinating N atoms in bold italic) of the chelate significantly smaller than that of triazolylpyridyl (2.60 and 2.77 Å, respectively).

Determination of the Binding Constants. The titration experiments by both absorbance and fluorescence measurements with the preferred cation for each glycoligand were then performed in acetonitrile (Figures 8 and 9). For **L1**, **L1′**, **L2**, and **L2′**, as the concentration of Ni^{II} (for **L1** and **L1′**) or Cu^{II} (for **L2** and **L2′**) increased, the fluorescence intensity was gradually quenched. The corresponding titration curves were well-fitted with a 1:1 complexation equation model (eq 1).[20,29] The values of the logarithm of their binding constants are reported in Table 3.

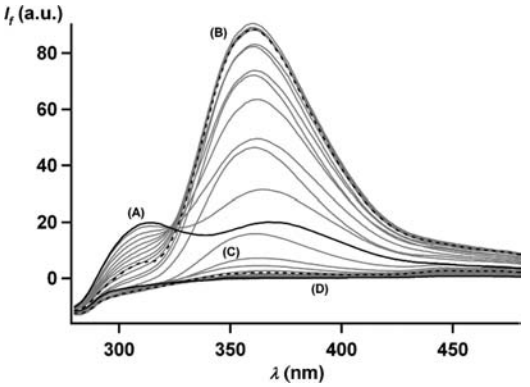

Figure 9. Fluorescence spectra obtained during titration of **L3** in acetonitrile ($C = 8 \times 10^{-6}$ mol L^{-1}) with $Cu(ClO_4)_2$ (from 0 to 5 equiv): (A) 0, (B) 0.5, (C) 1, and (D) 5 equiv of Cu^{II}. λ_{ex} = 260 nm.

Figure 10. Possible structures of copper(II) glyco complexes of **L3** and **L3′** in acetonitrile that could lead to the fluorescence plot profile measured by titration.

In the particular case of **L3** and **L3′**, a different fluorescent pattern was observed (Figure 9). From 0 to 0.5 equiv of Cu^{II}, the fluorescence of the excimer band at 370 nm was enhanced, whereas that of the monomer band at 320 nm was slightly quenched. Then, after 0.5 equiv, both emission bands were quenched. The plot of the fluorescence intensity of the excimer and monomer bands depending on the concentration of Cu^{II} revealed several equilibria (Figures 9 and S13 in the Supporting Information). A global analysis of the evolution of all absorption and fluorescence spectra using the *SPECFIT* Global Analysis System V3.0 indicated successive equilibria with 1:2 (M/L), 1:1 (M/L), or 2:2 (M/L) stoichiometries for complexation.[22] The logarithms of the binding constants of the (M/L) complex for both **L3** and **L3′** are reported in Table 3 for comparison.

Interestingly enough, this original behavior can be rationalized by considering the previously presented X-ray structure of the copper(II) complex of **L3**:[11] the structure presents a double-deck dimeric complex M_2L_2. As shown by the speciation diagrams obtained from the *SPECFIT* software (Figures S12 and S14 in the Supporting Information), the first step is the formation of a ML_2 complex from 0 to 0.5 equiv of Cu^{II}. From 0.5 to 1 equiv and further, ML (in the case of **L3**) and M_2L_2 (in the case of **L3′**) became the predominant species. For the ML_2 complex, the presence of an excimer band, with exaltation of the fluorescence intensity, can be attributed to π stacking of the uncoordinated claws (Figure 10). In the case of the M_2L_2 or ML complexes, the fluorescence of the claws is quenched because of coordination to Cu^{II}. To test this hypothesis, high-resolution electrospray mass spectra at the different stoichiometries of Cu^{II}, that is, 0, 0.5,

and 1 equiv, were performed in acetonitrile. The peaks at m/z 955.2928 and 509.1116 ($[M]^+$) for respectively solutions containing **L3**/Cu^{II} (2:1) and **L3**/Cu^{II} (2:2) in acetonitrile show the presence of all of the hypothesized species at the corresponding stoichiometry (see also the Supporting Information for **L3′**).

As can be seen from the binding constants in Table 3, the triazolylbenzothiadiazolyl claw appended twice in **L1** and **L1′** is not as efficient as the triazolylpyridyl claw appended also twice in **L3** and **L3′**. **L2** and **L2′**, showing a mixed coordination sphere, display the same selectivity as **L3** and **L3′**, with a preference for Cu^{II}. The more powerful coordinating chelate, that is, the triazolylpyridyl chelate, imposes its selectivity for Cu^{II}. The triazolylbenzothiadiazolyl claw, with its visible fluorescence emission, is thus a useful fluorescent reporter of complexation: on the one hand, it participates in the coordination sphere without changing the coordination selectivity of the triazolylpyridyl claw and, on the other hand, it allows a fluorescence study of complexation in the visible domain.

CONCLUSION

This article presents the synthesis of a novel series of glycoligands with fluorescence properties. A selective functionalization by various fluoroionophores was performed to tune glycoligands, demonstrating the potential versatility of the sugar platform. In the course of our studies about the implication of the furanose scaffold on the properties of complexation, intrinsically fluorescent glycoligands were shown to allow determination of the metal selectivity through competitive experiments and of binding constants using the fluorescence technique. Similar selectivities and binding constants were measured for the *xylo*-furanoses and the corresponding *ribo*-furanoses, indicating that the C3 configuration of furanose has no influence. Most importantly, the triazolylbenzothiadiazolyl claw was shown to be a convenient fluorescent reporter of complexation in the visible range without interfering in the binding and selectivity of the more efficient triazolylpyridyl claw. This result suggests the possible use of this triazolylbenzothiadiazolyl moiety as a passive fluorescent reporter of the coordinative properties of other moieties.

ASSOCIATED CONTENT

Supporting Information. X-ray crystallographic data for **L1** and **L2′** in CIF format, crystal data and structure refinement for **L1** and **L2′**, fluorescence and UV studies of **L1**, **L1′**, **L2**, **L2′**, **L3**, and **L3′** in acetonitrile, and mass analysis of copper complexes for **L3** and **L3′** in acetonitrile. This material is available free of charge via the Internet at http://pubs.acs.org.

AUTHOR INFORMATION

Corresponding Author

*E-mail: clotilde.policar@ens.fr. Fax: (+) 33-101 44 32 33 97.

ACKNOWLEDGMENT

Financial support was provided by the French Governement: ACI "Jeune Chercheur" 2004-J4044 (to C.P.).

REFERENCES

(1) Gruner, S. A. W.; Locardi, E.; Lohof, E.; Kessler, H. *Chem. Rev.* **2002**, *102*, 491–514.

(2) Dhungana, S.; Harrington, J. M.; Gebhardt, P.; Moellmann, U.; Crumbliss, A. L. *Inorg. Chem.* **2007**, *45*, 8362–8371.

(3) Diéguez, M.; Pàmies, O.; Ruiz, A.; Diaz, Y.; Castillon, S.; Claver, C. *Coord. Chem. Rev.* **2004**, *248*, 2165–2192.

(4) Storr, T.; Merkel, M.; Song-Zhao, G. X.; Scott, L. E.; Green, D. E.; Bowen, M. L.; Thompson, K. H.; Patrick, B. O.; Schugar, H. J.; Orvig, C. *J. Am. Chem. Soc.* **2007**, *129*, 7453–7463.

(5) Bellot, F.; Hardré, R.; Pelosi, G.; Thérisod, M.; Policar, C. *Chem. Commun.* **2005**, 5414–5417.

(6) Cisnetti, F.; Guillot, R.; Thérisod, M.; Policar, C. *Acta Crystallogr., Sect. C: Cryst. Struct. Commun.* **2007**, *C63*, m201–m203.

(7) Cisnetti, F.; Guillot, R.; Ibrahim, N.; Lambert, F.; Thérisod, M.; Policar, C. *Carbohydr. Res.* **2008**, *343*, 530–535.

(8) Damaj, Z.; Cisnetti, F.; Dupont, L.; Henon, E.; Policar, C.; Guillon, E. *Dalton Trans.* **2008**, 3235–3245.

(9) Charron, G.; Bellot, F.; Cisnetti, F.; Pelosi, G.; Rebilly, J.; Rivière, E.; Barra, A.; Mallah, T.; Policar, C. *Chem.—Eur. J.* **2007**, *13*, 2774–2782.

(10) Cisnetti, F.; Guillot, R.; Thérisod, M.; Desmadril, M.; Policar, C. *Inorg. Chem.* **2008**, *47*, 2243–2245.

(11) Garcia, L.; Maisonneuve, S.; Xie, J.; Guillot, R.; Rivière, E.; Desmadril, M.; Lambert, F.; Policar, C. *Inorg. Chem.* **2010**, *49*, 7282–7288.

(12) Lytle, C. M.; Lytle, F. W.; Yang, N.; Qian, J.; Hansen, D.; Zayed, A.; Terry, N. *Environ. Sci. Technol.* **1998**, *32*, 3087–3093.

(13) Loutseti, S.; Danielidis, D. B.; Economou-Amilli, A.; Katsaros, C.; Santas, R.; Santas, P. *Bioresour. Technol.* **2009**, *100*, 2099–2105.

(14) Hancock, R. D.; Martell, A. E. *Chem. Rev.* **1989**, *89*, 1875–1914.

(15) Hegetschweiler, K. *Chem. Soc. Rev.* **1999**, *28*, 239–249.

(16) Wolkenberg, S. E.; Boger, D. L. *Chem. Rev.* **2002**, *102*, 2477–2495.

(17) Lauffer, R. B. *Chem. Rev.* **1987**, *87*, 901.

(18) Valeur, B.; Leray, I. *Coord. Chem. Rev.* **2000**, *205*, 3–40.

(19) Bronson, R. T.; Bradshaw, J. S.; Savage, P. B.; Fuangswasdi, S.; Lee, S. C.; Krakowiak, K. E.; Izatt, R. M. *J. Org. Chem.* **2001**, *66*, 4752–4758.

(20) Maisonneuve, S.; Fang, Q.; Xie, J. *Tetrahedron* **2008**, *64*, 8716–8720.

(21) David, O.; Maisonneuve, S.; Xie, J. *Tetrahedron Lett.* **2007**, *48*, 6527–6530.

(22) Souchon, V.; Maisonneuve, S.; David, O.; Leray, I.; Xie, J.; Valeur, B. *Photochem. Photobiol. Sci.* **2008**, *7*, 1323–1331.

(23) Martinez, R.; Zapata, F.; Caballero, A.; Espinosa, A.; Tarraga, A.; Molina, P. *Org. Lett.* **2006**, *8*, 3235–3238.

(24) Kaur, S.; Kumar, S. *Tetrahedron Lett.* **2004**, *45*, 5081–5085.

(25) Zheng, Y.; Gattas-Asfura, K. M.; Konka, V.; Leblanc, R. M. *Chem. Commun.* **2002**, 2350–2351.

(26) Mei, Y.; Bentley, P. A.; Wang, W. *Tetrahedron Lett.* **2006**, *47*, 2447–2449.

(27) Sheldrick, G. M. *SHELXS-97*; Universität Göttingen: Göttingen, Germany,1997.

(28) Sheldrick, G. M. *SHELXL-97*; Universität Göttingen: Göttingen, Germany, 1997.

(29) Valeur, B. *Molecular Fluorescence. Principles and applications*; Wyley-VCH: Weinheim, Germany, 2002.

(30) Souchon, V.; Leray, I.; Valeur, B. *Chem. Commun.* **2006**, 4224–4226.

(31) Gampp, H.; Maeder, M.; Meyer, C. J.; Zuberbühler, A. D. *Talanta* **1985**, *32*, 95–101.

(32) Kolb, H. C.; Finn, M. G.; Sharpless, K. B. *Angew. Chem., Int. Ed.* **2001**, *40*, 2004–2021.

(33) Rostovtsev, V. V.; Green, L. G.; Fokin, V. V.; Sharpless, K. B. *Angew. Chem., Int. Ed.* **2002**, *41*, 2596–2599.

(34) Thanh Le, G.; Abbenante, G.; Becker, B.; Grathwohl, M.; Halliday, J.; Tometzki, G.; Zuegg, J.; Meutermans, W. *Drug Discovery Today* **2003**, *8*, 701–709.

(35) Kolb, H. C.; Sharpless, K. B. *Drug Discovery Today* **2003**, *8*, 1128–1137.

(36) Akhtaruzzaman, M.; Tomura, M.; Nishida, J.; Yamashita, Y. *J. Org. Chem.* **2004**, *69*, 2953–2958.

(37) Mindt, T. L.; Struthers, H.; Brans, L.; Anguelov, T.; Schweinsberg, C.; Maes, V.; Tourwe, D.; Schibli, R. *J. Am. Chem. Soc.* **2006**, *128*, 15096–15097.

(38) Colasson, B.; Save, M.; Milko, P.; Roithova, J.; Schroder, D.; Reinaud, O. *Org. Lett.* **2007**, *9*, 4987–4990.

(39) This exaltation of fluorescence is of interest. Nevertheless, as indicated in the following paragraph, the competition between Cu^{II} and

either Zn^{II} or Cd^{II} unambiguously showed a preference for Cu^{II} because 5 equiv of this cation is sufficient to induce copper complexation in the presence of 50 equiv of Zn^{II} and Cd^{II} (see Figure 7).

(40) Bodenant, B.; Weil, T.; Businelli-Pourcel, M.; Fages, F.; Barbe, B.; Pianet, I.; Laguerre, M. *J. Org. Chem.* **1999**, *64*, 7034–7039.

(41) Zheng, Y.; Huo, Q.; Kele, P.; Andreopoulos, F. M.; Pham, S. M.; Leblanc, R. M. *Org. Lett.* **2001**, *3*, 3277–3280.

(42) Roy, B. C.; Chandra, B.; Hromas, D.; Mallik, S. *Org. Lett.* **2003**, *5*, 11–14.

(43) Klein, G.; Kaufmann, D.; Schürch, S.; Reymond, J. *Chem. Commun.* **2001**, 561–562.

(44) Shannon, R. D. *Acta Crystallogr.* **1976**, *A32*, 751–767.